Talanta 123 (2014) 161–168

Contents lists available at ScienceDirect

Talanta

journal homepage: www.elsevier.com/locate/talanta

Highly sensitive immunoassay based on SERS using nano-Au immune probes and a nano-Ag immune substrate

Lei Shu [a], Jun Zhou [a,*], Xiaocong Yuan [b], Lucia Petti [c], Jinping Chen [a], Zhenhong Jia [d], Pasquale Mormile [c]

[a] Institute of Photonics, Faculty of Science, Ningbo University, Ningbo 315211, China
[b] Institute of Micro & Nano Optics, Shenzhen University, Shenzhen 518060, China
[c] Institute of Cybernetics "E. Caianiello" of CNR, Via Campi Flegrei 34, 80072 Pozzuoli, Italy
[d] College of Information Science and Engineering, Xinjiang University, Urumqi 830046, China

ARTICLE INFO

Article history:
Received 6 November 2013
Received in revised form
27 January 2014
Accepted 2 February 2014
Available online 14 February 2014

Keywords:
Immunoassay
Surface-enhanced Raman scattering
Biosensing
Nanoparticle
SERS substrate

ABSTRACT

A super-high-sensitivity immunoassay based on surface-enhanced Raman scattering (SERS) was implemented using the nano-Au immune probes and nano-Ag immune substrate. Ultraviolet–visible extinction spectra, transmission electron microscopy (TEM) and scanning electron microscopy (SEM) images, and SERS spectra were used to characterise the nano-Au immune probes and the nano-Ag immune substrate. The nano-Ag immune substrate was prepared by the *in situ* growth of Ag nanoparticles and the subsequent linkage of these nanoparticles with anti-apolipoprotein B on a silicon wafer. The nano-Ag immune substrate exhibited strong SERS activity, excellent reproducibility, and high biospecificity. The nano-Au immune probes were prepared by immobilising 4-mercaptobenzoic acid (4MBA) molecules as a Raman reporter and anti-apolipoprotein B onto the surfaces of Au nanoparticles. It was found that 4MBA induced the aggregation of Au nanoparticles, resulting in the generation of vast hot spots. Moreover, the nano-Au immune probes exhibited strong SERS activity and high biospecificity. A sandwich-type immunoassay structure consisting of the nano-Au immune probes and nano-Ag immune substrate was used to detect the concentration of apolipoprotein B, where the detection limit was as low as 2 fg/mL (3.878×10^{-18} mol/L). Taken together, the experimental results indicate that the proposed immunoassay protocol has a great potential application in biological sensing and clinical diagnostics.

1. Introduction

Since the surface-enhanced Raman scattering (SERS) phenomenon was observed for the first time in the Raman scatter experiment of pyridine adsorbed on a silver electrode in 1974 [1], SERS has attracted much of the attention of scientists, who have sought to explore its mechanism and application theoretically and experimentally [2]. Because the noble metals (*e.g.*, gold, silver and copper) with nanoscale features exhibit electromagnetic and chemical enhancement, the scattering cross-sections of target molecules residing at or near the surfaces of the noble metals can be enhanced by factors of up to $\sim 10^{14}$ [3–6], which enables single molecule detection [7]. As a powerful tool, SERS technology has been widely applied in various disciplines, such as analytical chemistry [8], life sciences [9], and environmental science [10].

SERS-based immunoassays, in particular, have a number of advantages over fluorescence-based assays in terms of photostability and multiplexed detection [11,12]. In general, label-free direct detection [13,14] and Raman reporter-labelled indirect detection are the two major assay techniques used with SERS-based immunoassays [15,16]. In the direct method, the detection of the SERS signal of the target protein is performed using Au nanoparticles (AuNPs) or Ag nanoparticles (AgNPs) as the SERS substrate while in the indirect method, the SERS signal of the Raman reporter molecules linked to the target protein is detected. As in the case of enzyme-linked immunosorbent assay (ELISA), a sandwich immunoassay structure consisting of the immune probes/target protein/immune substrate is constructed via the specific immunoreaction between the antigen and the antibody [17,18]. The target proteins can be analysed qualitatively or quantitatively via the SERS spectrum of the Raman reporter molecule. The indirect strategy is a practical and powerful method for performing highly sensitive immunoassays because the SERS scattering cross-sections and SERS signals of the Raman reporter molecules are high in magnitude.

* Corresponding author. Tel.: +86 574 8760 0794; fax: +86 574 8760 0744.
E-mail address: zhoujun@nbu.edu.cn (J. Zhou).

http://dx.doi.org/10.1016/j.talanta.2014.02.015
0039-9140

In the indirect immunoassay, AuNPs or AgNPs are used to prepare the immune probes and the immune substrate owing to their long-term stability, controllable size distributions, good biocompatibility, and, specifically, their excellent SERS enhancement effects [19,20]. The immune probes are prepared by immobilising the recognition antibody and the Raman reporter molecule on the AuNPs or AgNPs. While preparing the immune probes, an aggregation agent, such as acidified sulphate, organic Raman labels molecules, and positively charged polymers, is often used to induce the random aggregation of AuNPs or AgNPs. This is because the response of SERS-based immunoassays is critically related to the size and degree of aggregation of the AuNPs or AgNPs [11,21]. Typically, the SERS signal obtained from aggregated nanoparticles is larger than that obtained from isolated nanoparticles [5,22]. This is because when the AuNPs or AgNPs form aggregates, their transition dipoles couple with each other, resulting in a significant enhancement of the SERS effect at the nanoscale gaps ("hot spots") between the aggregated nanoparticles [23,24]. To improve the detection sensitivity of SERS-based immunoassays, numerous efforts have been made to prepare immune probes with aggregated nanoparticles by adding aggregation agents. For example, Cui et al. [18] reported a SERS-based immunoassay in which strong signals were obtained from aggregated AuNPs whose aggregation was induced by 4-mercaptobenzoic acid (4MBA). Su et al. [25] synthesised new types of Raman tags called composite organic–inorganic nanoparticles (COINS) for multiplex and ultrasensitive immunoassays.

The bottom layer of the sandwich immunoassay structure is a substrate immobilised with a capture antibody. In traditional immunoassays, the substrate, such as silicon wafer and glass/quartz slide, is usually coated by polylysine for immobilising the capture antibody [20,26]. However, the SERS-active substrate, which is constructed by directly assembling AuNPs or AgNPs on the substrate, is increasingly used in immunoassays, as reported in Ref. [18], because AuNPs and AgNPs have an excellent SERS enhancement effect. In addition, the SERS-active immune substrate and immune probes can form together a two metal layers structure via an immnuoreaction, and a large amount of SERS "hot spots" may emerge in the metal nanoparticle aggregates between the two metal layers [27] to increase the sensitivity of the SERS-based immunoassay.

In this study, a super-high-sensitivity immunoassay based on SERS was implemented using the nano-Au immune probes and nano-Ag immune substrate. The nano-Au immune probes were formed by immobilising 4MBA, anti-apolipoprotein B (anti-apoB), and a blocking agent (bovine serum albumin or BSA) on the surfaces of the AuNPs. In addition to the use as a Raman reporter molecule, 4MBA can be used also as an aggregation agent to induce the aggregation of AuNPs, thereby resulting in an improvement in the sensitivity of the immunoassay. In addition, Ag ions were reduced into AgNPs via Si–H bonds, and these AgNPs were covered on a silicon wafer to form the SERS active substrate [28]. Next, anti-apoB and BSA were immobilised on the SERS-active substrate to form the nano-Ag immune substrate which exhibited specific binding with apolipoprotein B (apoB). Subsequently, the ELISA protocol was referenced to construct the sandwich immunoassay structure of the nano-Au immune probes/target antigen/nano-Ag immune substrate via an immunoreaction between the antibody and antigen. Here, the apoB is the target antigen to be detected because the concentration of apoB is a superior index for determining the risk of cardiovascular disease [29]. The detection limit in our immunoassay experiment was as low as 2 fg/mL (3.878×10^{-18} mol/L). Comparing the recent works, for example, Zhu et al. demonstrated a competitive SERS immunoassay for detection of clenbuterol at a low concentration (~0.1 pg/ml) [30], and Martinez-Perdiguero et al. presented the sandwich surface plasmon resonance immunoassay for the detection of the TNF-alpha protein in human serum at a low concentration (54.4 pg/mL) [31]; our immunoassay protocol has got a lower limit of detection due to the aggregation of AuNPs inducing more SERS "hot spots" in the sandwich structure consisting of nano-Au immune probes and nano-Ag immune substrate. Thus, our method may be used to measure the minute changes in the concentration of apoB for the prevention and early treatment of cardiovascular disease.

2. Materials and methods

2.1. Reagents

Hydrogen tetrachloroaurate (III) trihydrate ($HAuCl_4 \cdot 3H_2O$) and silver nitrate ($AgNO_3$) were purchased from Sigma-Aldrich; 4-mercaptobenzoic acid was obtained from J&K Scientific Ltd. Rhodamine 6G (Rh6G) was obtained from Sinopharm Chemical Reagent Co. (Shanghai, China). Sodium citrate was purchased from Bodi Chemical Reagents Co. (Tianjin, China). ApoB and anti-apoB were obtained from Ningbo Rui Bio-technology Co., Ltd. Bovine serum albumin (BSA) was purchased from NanJing SunShine Biotechnology Co., Ltd. Hydrogen fluoride (HF) was purchased from Wuxi Chenyang Chemical Co., Ltd. Phosphate buffer solution (PBS, pH 7), Tris-buffered saline (TBS, pH 7.6), and TBS/0.05% Tween20 buffer solution (0.05 M Tris, 0.138 M NaCl, 0.0027 M KCl, 0.05% Tween®20, pH 8) were purchased from Sigma-Aldrich. Milli-Q water (resistivity of 18.2 MΩ cm) was used to prepare all solutions. The glassware was cleaned with aqua regia and rinsed with deionised water several times prior to the experiments.

2.2. Preparation of the 4MBA-labelled immune nano-Au probes

The 4MBA-labelled nano-Au immune probes were prepared by a process that consisted of the following four steps. First, an Au colloid was prepared according to the procedure developed by Turkevich et al. [32]. Two millilitres (1%) sodium citrate aqueous solution was added immediately to 100 mL of a 10^{-4} g/mL $HAuCl_4$ boiling solution under vigorous stirring. The mixture was stirred vigorously and boiled for an additional 20 min. Second, the aggregation of 4MBA-labelled AuNPs was prepared by the following process: 3 mL of Au colloid was washed by centrifugation at 11,000 rpm for 30 min, the clear supernatant was removed, and the sedimented AuNPs were resuspended in 3 mL of deionised water. Next, 8 μL of 1 mM 4MBA (in ethanol) was added to the Au colloid under vigorous stirring, and the mixture was incubated at room temperature for 12 h. Next, the mixture was washed by centrifugation at 11,000 rpm for 30 min to remove the excess 4MBA; the clear supernatant was removed and the sedimented AuNPs were resuspended in 3 mL of deionised water. This process was repeated two times. Subsequently, the sedimented 4MBA-labelled AuNPs were suspended in 1 mL of PBS under ultrasonic oscillation. Third, the anti-apoB was immobilised on the 4MBA-labelled AuNPs via static and hydrophobic interactions [20]. Twenty microlitres (2 mg/mL) anti-apoB in PBS was added to 1 mL of the 4MBA-labelled AuNPs solution, and the mixture was incubated at 4 °C for 1.5 h. The mixture was then washed by centrifugation twice at 11,000 rpm for 30 min to remove the excess anti-apoB. Finally, 10 μL of 3% BSA solution in PBS was added to the 4MBA-labelled immune AuNPs to shield the bare sites on the surfaces of the AuNPs. After incubation at room temperature for 1 h, the mixture was washed twice by centrifugation at 11,000 rpm for 30 min to remove the excess BSA. Next, the sediment was resuspended in 1 mL of PBS under ultrasonic oscillation, and the 4MBA-labelled immune nano-Au probes were finally obtained.

2.3. Preparation of the SERS-active immune substrate

The SERS-active immune substrate was prepared according to the following three steps. In the first step, AgNPs were deposited onto the surface of a silicon wafer through the reduction of Ag ions via S–H bonds [27]. Initially, the silicon wafer was ultrasonically cleaned with acetone for 30 min and with deionised water for 10 min, and then dried using argon gas. After the ultrasonic treatment, the Si wafer was immersed in an oxidant solution containing H_2SO_4 (98%) and H_2O_2 (30%) in a volume ratio of 3:1 for 40 min. Next, the Si wafer was washed thrice with deionised water to remove all organics from its surface and dried with argon gas. Next, the cleaned Si wafer was immersed in an aqueous solution of hydrogen fluoride (HF, 10%) for 40 min, resulting in the surface of the wafer becoming H-terminated, thus, becoming covered with Si–H bonds. The H-terminated Si wafer was then immediately immersed into a freshly prepared silver nitrate ($AgNO_3$, 2%) solution while being stirred slowly for 1 min. The Ag ions in the solution were reduced to AgNPs via the Si–H bonds, and the AgNPs covered the surface of the Si wafer, resulting in the SERS-active substrate. This SERS-active substrate was then dried with a gentle flow of argon gas. In the second step, a monolayer of anti-apoB was immobilised onto the SERS-active substrate. Thirteen microlitres (2 mg/mL) anti-apoB in PBS was pipetted onto the substrate, and immobilisation was subsequently performed at 4 °C in an environment with a relative humidity of 60% over a period of 12 h. Next, the substrate was washed successively with TBS/0.05% Tween20 buffer solution, TBS, and deionised water to remove any residual protein from its surface, and dried in a gentle flow of argon gas. In the third step, the nonspecific adsorption sites on the surface of the substrate were blocked via treatment with a blocking solution (3% BSA in PBS) for 3 h at room temperature. Next, the prepared SERS-active immune substrate was successively washed with TBS/0.05% Tween®20 buffer solution, TBS, and deionised water to remove the residual BSA and dried in a gentle flow of argon gas. Finally, the prepared SERS-active immune substrate was stored at 4 °C for further analyses.

2.4. Immunoassay protocol

The immunoassay was performed according to the ELISA sandwich protocol, as shown in Fig. 1. Briefly, 13 μL of the apoB solution was dripped onto the prepared SERS-active immune substrate, and then incubated at 37 °C for 2 h. The incubation temperature was set to 37 °C for binding of the anti-apoB and the apoB at an approximate temperature of human body. After the completion of the immunoreaction between anti-apoB and apoB, the substrate was rinsed successively with TBS/0.05% Tween®20 buffer solution, TBS, and deionised water to remove any residual antigen that was not captured by the antibody on the SERS-active immune substrate. Next, each sampling point was covered with 13 μL of the 4MBA-labelled immune Au probes solution, and then incubated at 4 °C for 2 h. The substrate was then rinsed with TBS/0.05% Tween®20 buffer solution, TBS, and deionised water. Finally, the substrate was dried in a gentle flow of argon gas and stored at 4 °C.

2.5. Instrumentation

Transmission electron microscopy (TEM) images characterising the morphologies of the immune nano-Au probes were obtained using transmission electron microscopy (JEM-2100F, JEOL) at 200 kV accelerating voltage. The prepared AuNPs, 4MBA-labelled AuNPs and 4MBA-labelled immune nano-Au probes solution were dripped on TEM grids and dried in a gentle flow of argon gas, and then the samples were used for TEM measurement. The scanning electron microscopy (SEM) images characterising the morphologies of the SERS-active substrate were obtained using field-emission scanning electron microscopy (SU-70, Hitachi) with 10 kV accelerating voltage. A UV–vis spectrometer (TU-1901, Pgeneral) was used to monitor the formation of the 4MBA-labelled immune nano-Au probes. A high-speed centrifuge (TGL-20M, Shanghai Lu Xiangyi Centrifuge Instrument Co. Ltd) was used for sample purification. The SERS signals were measured using a Raman spectrometer (BWS415, B&W Tek Inc.). The specifications of the Raman spectrometer are established as the following: a semiconductor laser with 785 nm radiation wavelength was used as the excitation source; the laser power at the sample position was 49.55 mW and the accumulation time was 10 s. The scattered radiation was collected using a 40× objective lens with numerical aperture (NA) 0.65, dispersed by the grating of 1200 lines/mm, and then passed through a slit of 20 μm width to the charge-coupled device (CCD, 2048 × 2048 pixels) detector.

3. Results and discussion

3.1. Characterisation of the 4MBA-labelled immune nano-Au probes

The UV–vis spectra were used to monitor the characteristics of the 4MBA-labelled immune nano-Au probes during the various stages of the preparation process, as shown in Fig. 2. The surface

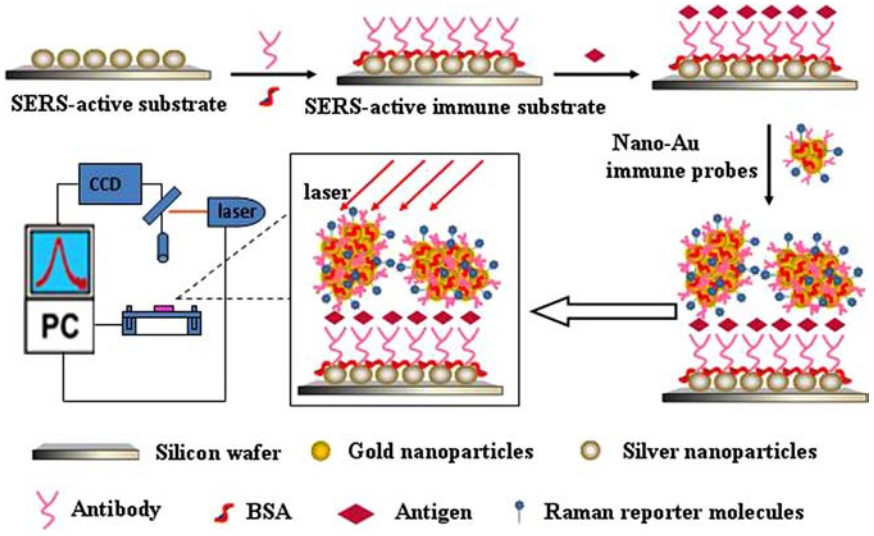

Fig. 1. Schematic representation of the protocol for the SERS-based immunoassay.

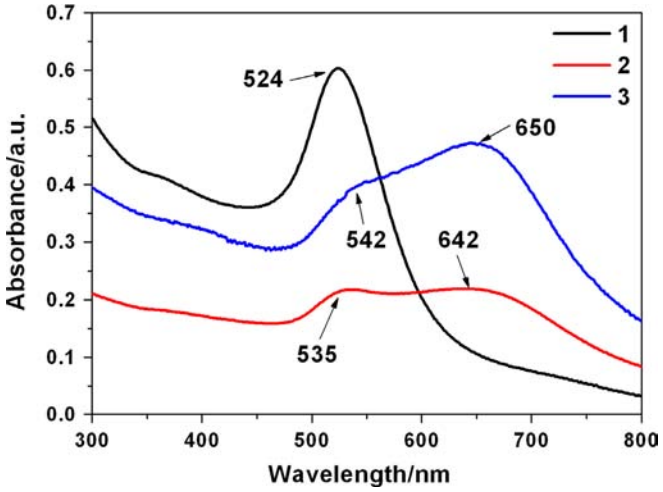

Fig. 2. Extinction spectra of the citrate–AuNPs (curve 1, upper), 4MBA-labelled AuNPs (curve 2, lower) and 4MBA-labelled immune nano-Au probes (curve 3, center). (For interpretation of the references to colour in this figure, the reader is referred to the web version of this article.)

plasma resonance band of the citrate-capped AuNPs demonstrated a maximum at 524 nm and a narrow full width at half maximum (FWHM) (black curve shown in Fig. 2), which illustrated that the prepared AuNPs were monodisperse in the Au colloidal solution [33]. However, after the addition of 4MBA (1 mM in ethanol), the surface plasma resonance peak was red-shifted from 524 nm to 535 nm, a new broad extinction peak appeared on the red side of the spectrum, located at 642 nm as the red curve shown in Fig. 2. Cui et al. [17] reported that this red-shift of the surface plasma resonance peak corresponded to an increase in the size of the AuNPs, demonstrating that the binding of 4MBA to the surfaces of the AuNPs was successful. In fact, prior to the addition of 4MBA, the AuNPs were stable in the solution owing to the electrostatic repulsion between the negative surface charges formed by the citrate ions on the surfaces of the nanoparticles. However, after the addition of 4MBA, the citrate layers around the AuNPs were replaced by 4MBA molecules via a "place-exchange reaction" between the citrate ions and molecules. Thus, the 4MBA molecules were covalently adsorbed onto the surfaces of the AuNPs owing to the formation of S–Au bonds. Because the charges on the surfaces of the AuNPs are no longer sufficient to cause electrostatic

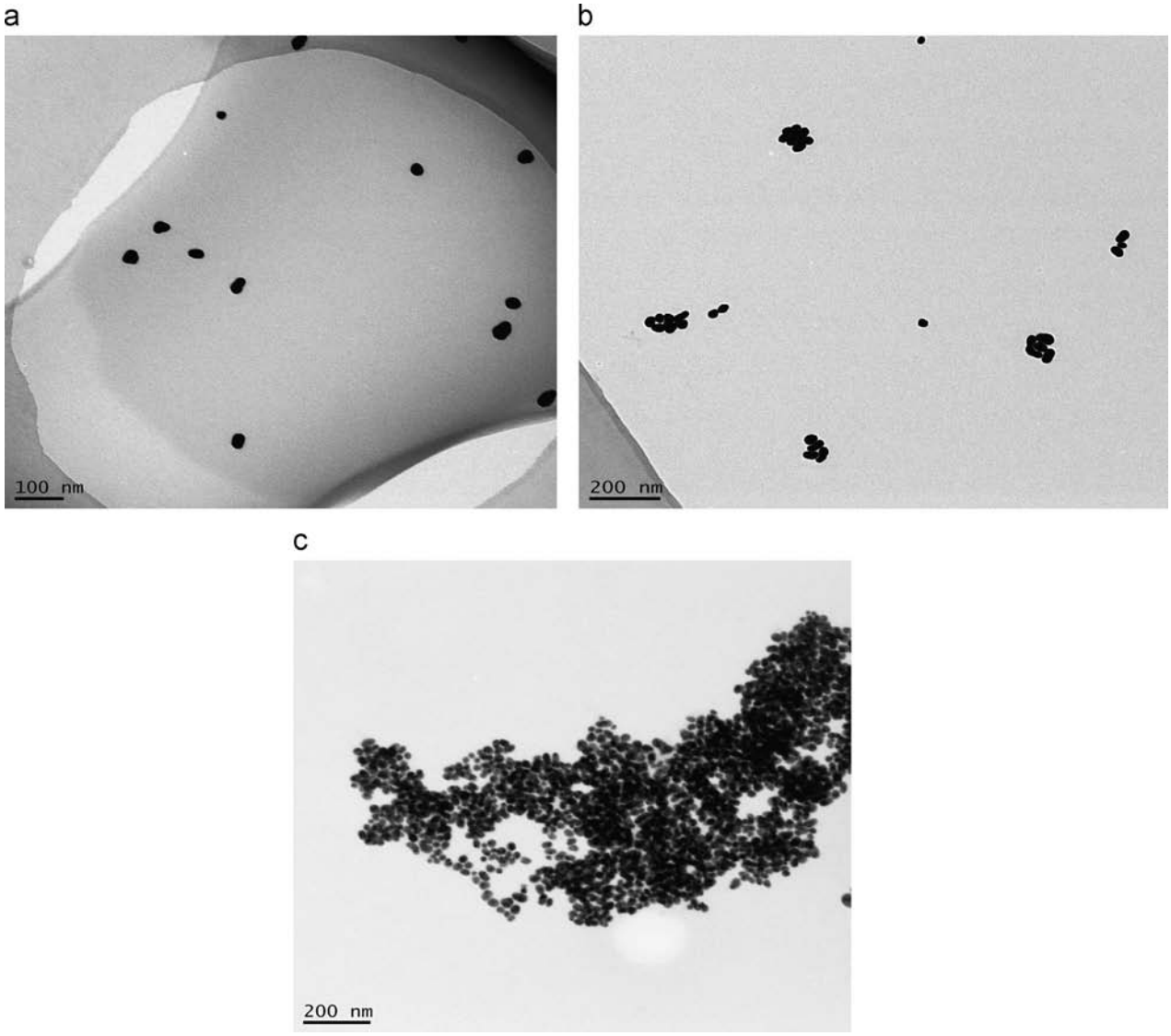

Fig. 3. TEM images of the 4MBA-labelled immune nano-Au probes during different stages of the preparation process: (a) TEM images of the colloidal AuNPs with a good monodispersity, (b) 4MBA-labelled AuNPs aggregates, and (c) the 4MBA-labelled immune nano-Au probes.

repulsion, the AuNPs aggregate after the place-exchange reaction. As the interparticle spaces decrease, the electrical dipole–dipole interactions and the coupling between neighbouring particles are induced in the aggregation of the AuNPs [34]. Thus, the extinction band at 642 nm originated from the plasmon resonance of the aggregated AuNPs after the addition of 4MBA [35,36]. After adding anti-apoB, the two extinction peaks were red-shifted from 535 nm to 542 nm and 642 nm to 650 nm (as the blue curve shown in Fig. 2). This finding indicated that the size of the aggregates further increased, which suggested that anti-apoB was successfully adsorbed onto the surfaces of the 4MBA-labelled AuNPs aggregates [34].

Moreover, the corresponding morphologies of the 4MBA-labelled immune nano-Au probes are shown by the TEM images in Fig. 3, which reveal the aggregation of AuNPs in the synthesis process. As shown in Fig. 3(a), the AuNPs were nearly spherical with an average size of ~24 nm by a count of 175 particles and exhibited good monodispersity without aggregation. However, after the addition of the Raman reporter 4MBA, the interparticle distances decreased, and the AuNPs formed aggregates, as shown in Fig. 3(b). After the anti-apoB bound to the 4MBA-labelled AuNPs aggregates, the size of the aggregates increased significantly, as shown in Fig. 3(c).

The SERS spectra of the 4MBA-labelled AuNPs aggregates and 4MBA-labelled immune nano-Au probes were measured under different conditions as shown in Fig. 4. In the case of solution phase, the SERS signal intensity of the 4MBA-labelled AuNPs aggregates was stronger than that of the 4MBA-labelled immune Au probes (see Fig. 4(a)). This finding suggests that, after the addition of anti-apoB, the immobilisation of the anti-apoB onto the surfaces of the 4MBA-labelled AuNPs does not induce further aggregation of the 4MBA-labelled AuNPs aggregates but the wider gaps between AuNPs to reduce the number of hot spots, which resulted in the decrease of the SERS signal intensity of the 4MBA-labelled immune Au probes. In the case of the solid phase, the same volumes (5 μL) of 4MBA-labelled AuNP aggregates and 4MBA-labelled immune nano-Au probe solution were dripped onto a clean quartz glass and then dried naturally. The SERS signal intensity of the 4MBA-labelled AuNPs aggregates and 4MBA-labelled immune nano-Au probes showed robust enhancement, particular for the latter probes, as shown in Fig. 4(b). This indicated that the number of hot spots in the solid phase demonstrated a significant increase compared with that of the solution phase. This was due to the immobilisation of anti-apoB, which caused a significant increase in the size of the AuNPs aggregates (see Fig. 3(c)) such that a greater number of hot spots were generated in the solid phase. Based on this observation, the detection sensitivity of the SERS-based immunoassays may be significantly improved in the solid phase.

3.2. Characterisation of the SERS-active substrate

It is well known that enhancement of the SERS-active substrate is critically correlated to the size and the aggregation degree of the

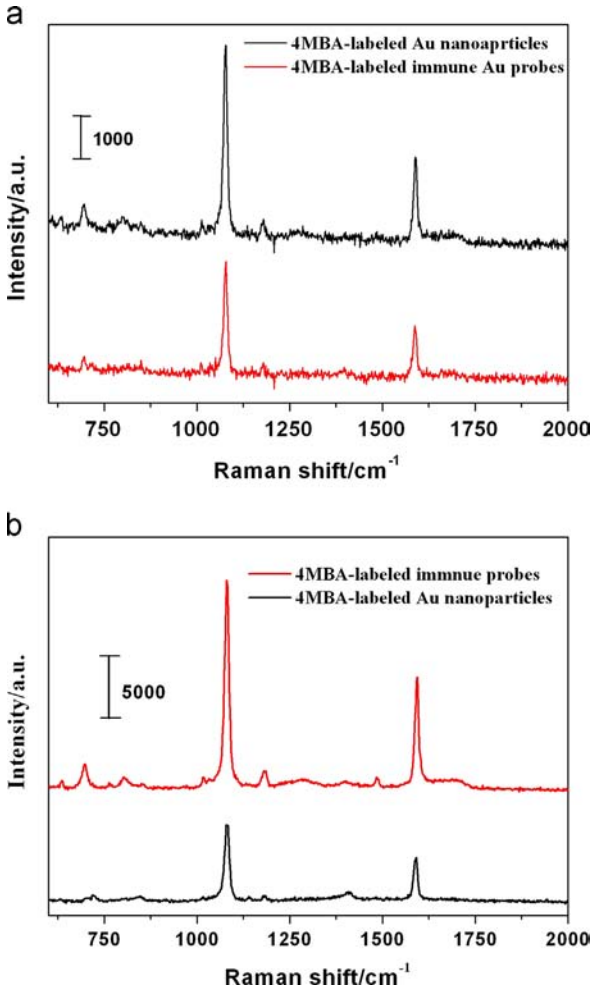

Fig. 4. SERS spectra of the 4MBA-labelled AuNPs aggregate and 4MBA-labelled immune nano-Au probes: (a) in the solution phase and (b) in the solid phase.

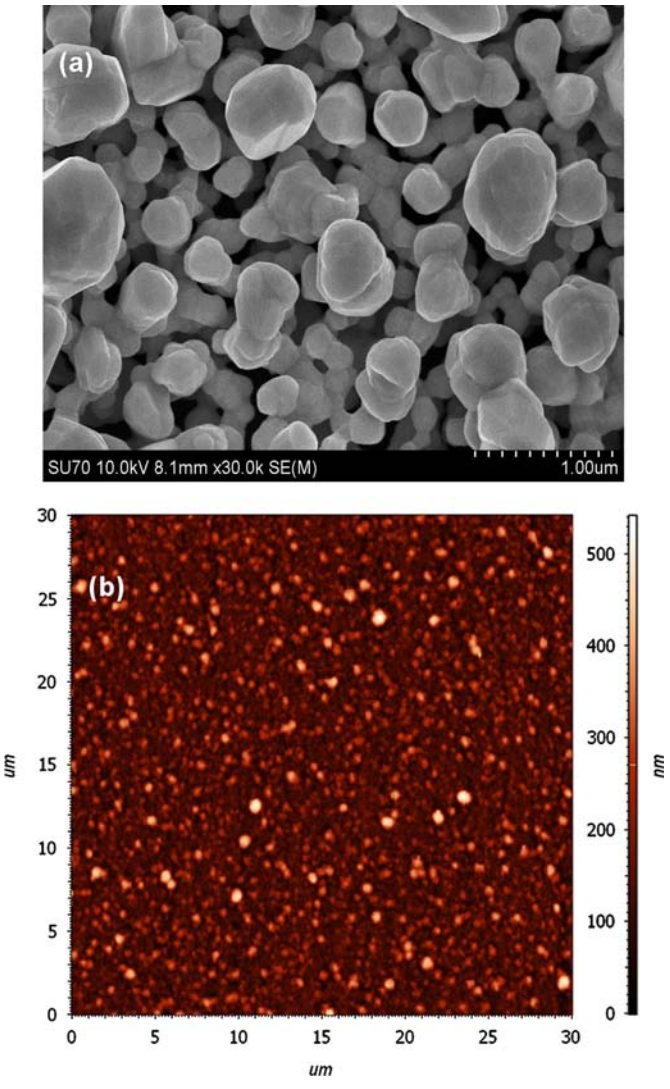

Fig. 5. (a) SEM and (b) AFM images of the prepared SERS-active substrate.

AgNPs [5,17,21]. In our experiment, the SERS-active substrate was synthesised via the *in situ* growth of AgNPs on the Si wafer substrate via an established HF etching-assisted chemical reduction method [28]. Moreover, the SEM and AFM images of the prepared SERS-active substrate, as shown in Fig. 5, indicated that the AgNPs with an average size of ~250 nm formed the aggregates covering the surface of Si wafer. In order to survey the SERS enhancement ability of the prepared substrate, its Raman enhancement factor (*EF*) is determined using the following equation [21]:

$$EF = \frac{I_{SERS} N_{bulk}}{I_{bulk} N_{SERS}}$$

where I_{SERS} and I_{bulk} are the intensities of the same Raman band in the SERS and bulk Raman spectra, respectively; N_{bulk} is the number of bulk molecules probed in the bulk sample; and N_{SERS} is the number of molecules adsorbed on the SERS-active substrate. In this study, the intensity of the peak at ~1078 cm^{-1}, as the strongest band corresponding to the ν (C–C) ring-breathing mode in the spectra, was used to estimate the values of *EF*. The Raman spectrum of the 4MBA solution (10 mM) was used to estimate the "bulk" values of the *EF*. $N_{bulk} = 1 \times 10^{13}$ was calculated using a 4MBA solution concentration at 10 mM and the illuminated volume was 1.66 μm^3. To obtain the value of N_{SERS}, the diameter of the illumination focus 1.473 μm was first calculated using the following equation: $D_{diameter} = (\lambda/NA) \times 1.22$ [37], in which the *NA* of the objective lens of the Raman spectrometer was 0.65 and the wavelength of the excitation laser was 785 nm. Next, the areal density was estimated using 5 μL of the 4MBA (10 mM) solution on the SERS-active substrate with 1 cm^2. We assumed that the 4MBA molecules were uniformly distributed on the SERS-active substrate, and thus, $N_{SERS} = 5.131 \times 10^8$. In addition, as shown in Fig. 6, the I_{SERS} and I_{bulk} values were 4×10^5 and 2.166×10^3, respectively. Thus, the *EF* value of the SERS-active substrate was calculated as 3.6×10^8.

To evaluate the reproducibility of the SERS-active substrate for the immunoassay, the substrate was immersed in a 1 mM R6G solution for 3 h. After the R6G molecules had been adsorbed on the AgNPs, the SERS-active substrate was washed with deionised water thrice to remove any residual R6G molecules and then dried in a gentle flow of argon gas. The SERS spectrum of the R6G molecules was recorded at 25 random spots on the substrate, as shown in Fig. 7(a). Fig. 7(b) presents the intensities of the SERS peak at 1514 cm^{-1}, which corresponds to the above 25 spots, and exhibits intensity values of ~6976 ± 772 with a relatively small standard deviation (11.1%). These results demonstrated the excellent SERS reproducibility of the SERS-active substrate due to the tightly immobilised AgNPs on the silicon wafer, which effectively prevented the random aggregation of nanoparticles.

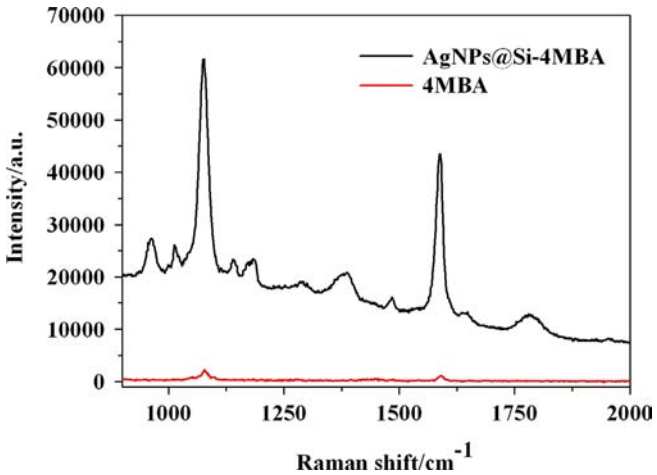

Fig. 6. The SERS spectrum of 4MBA collected from the SERS-active substrate and the normal Raman spectrum of 4MBA in solution under the same sampling conditions.

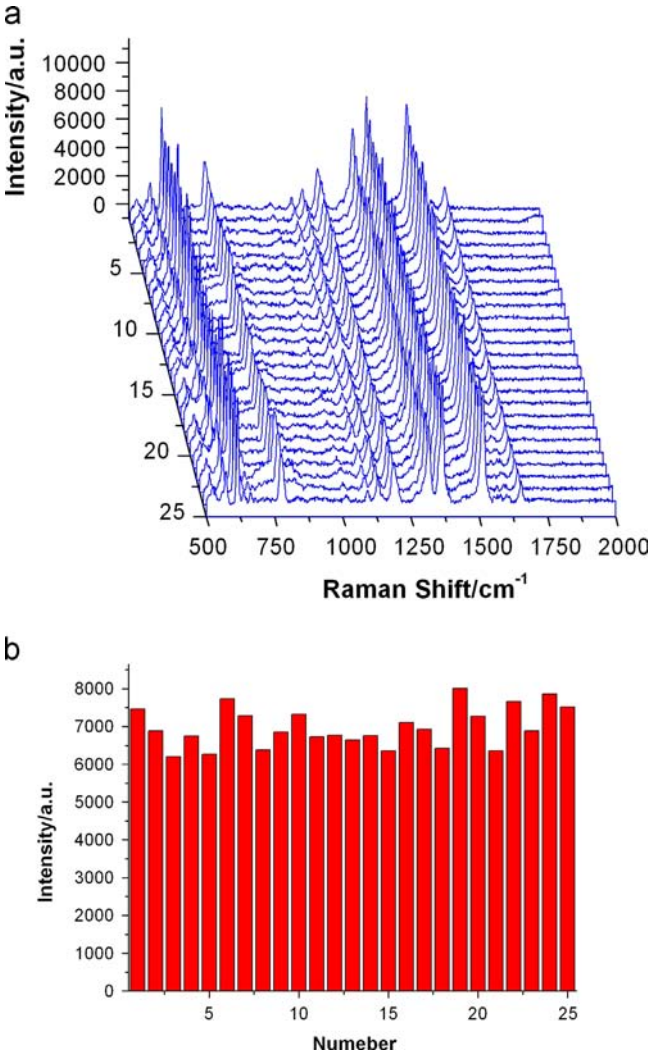

Fig. 7. (a) Raman spectra of R6G molecules absorbed on the SERS-active substrate and (b) the intensities of the peak at 1514 cm^{-1}.

3.3. Highly sensitive immunoassay

In this section, the SERS-active immune substrate and 4MBA-labelled immune nano-Au probes were used to perform a highly sensitive immunoassay. A "sandwich-type" structure was formed by exploiting the immune reaction between the target antigen and the SERS-active immune substrate as well as the reaction between the target antigen and 4MBA-labelled immune nano-Au probes. The established protocol, as shown in Fig. 1, was used for this purpose. The dependence of the SERS signal on the concentration of the apoB was investigated, and the detection limit of the concentrations of apoB in the SERS-based immunoassay was also determined. The SERS spectra of the 4MBA corresponding to the different concentrations of apoB are shown in Fig. 8(a). The concentration of apoB decreased from 200 pg/mL to 2 fg/mL, and the intensity of the SERS peak of 4MBA also gradually reduced. Each spectrum was recorded by averaging seven readings of the SERS singals at different points on the sample. The background without the apoB was also measured as the baseline, shown as the 0 fg/mL spectral line in Fig. 8(a). The intensity of the SERS peak in

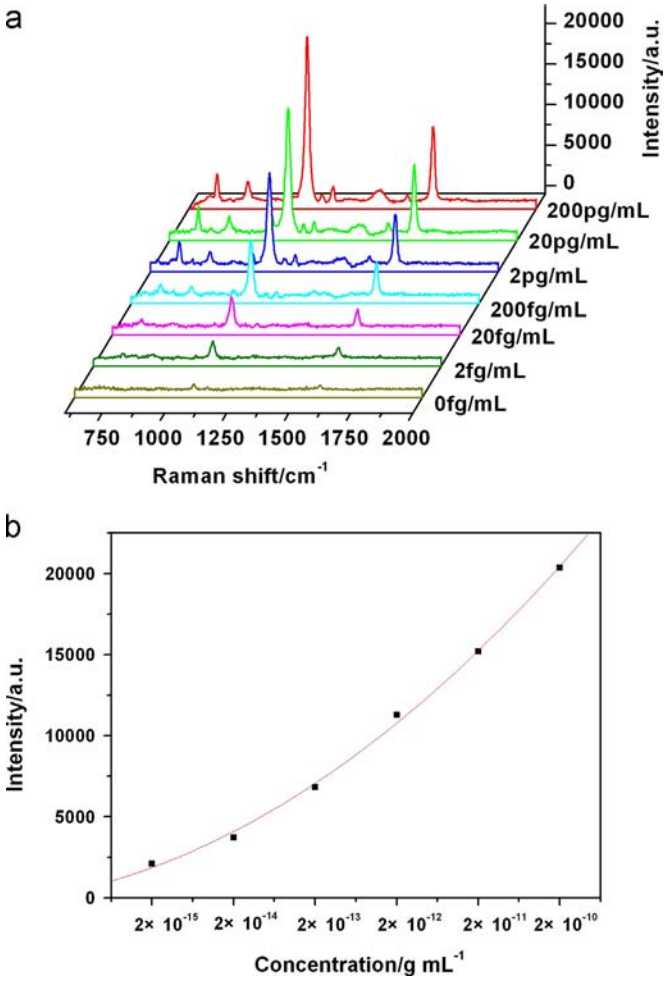

Fig. 8. (a) SERS spectra of 4MBA corresponding to the different concentrations of apoB and (b) the dose–response curve of the peak intensity at 1078 cm^{-1} changed with the concentration of apoB.

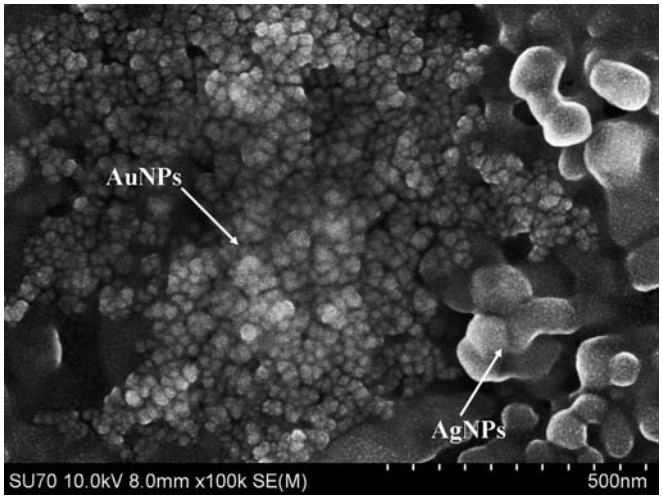

Fig. 9. SEM image of the sandwich structure consisted of the nano-Ag immune substrate and nano-Au immune probes.

the case of the apoB concentration of 2 fg/mL (~2120) was distinctly greater than that of the background (~659), demonstrating the super-high-sensitivity of the designed immunoassay. From Fig. 8(a), the dose–response fit curve of the peak intensity at 1078 cm^{-1} was obtained for the different concentrations of apoB,

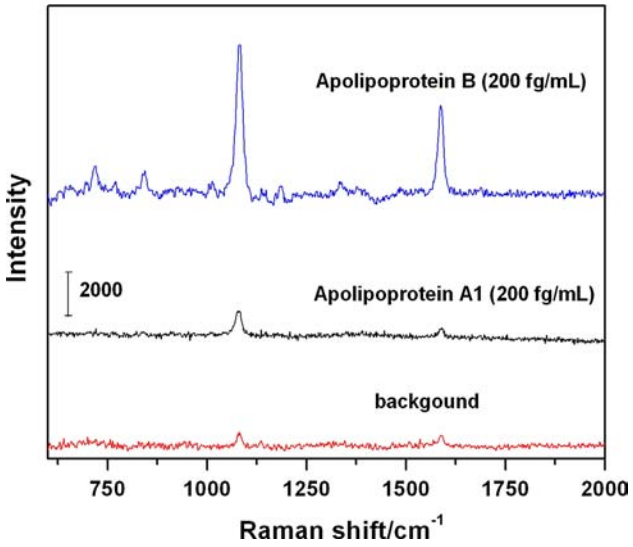

Fig. 10. SERS signal of 4MBA for the 200 fg/mL target antigens, which were apoB (blue line, upper) and apoA1 (black line, center), and the lower red line represents the SERS background. (For interpretation of the references to colour in this figure legend, the reader is referred to the web version of this article.)

with a quadratic fitting equation $y = 398.71027 + 1097.84722x + 374.27665x^2$. From the dose–response curve, the intensities of the SERS peak are approximately proportional to the concentration of the target antigen and the detection limit of the concentration of apoB is as low as 2 fg/mL (3.878×10^{-18} mol/L). The super-high sensitive immunoassay of apoB was derived from the advantage of the sandwich structure, which consisted of the SERS-active immune substrate and immune probes (as shown in Fig. 9). Thus, the metal nanoparticle aggregates between the bimetal nanoparticle layers can produce more SERS "hot spots", which enable the immunoassay of apoB to reach above detection limit.

In addition, the immunological specificity of the SERS-based immunoassay was also examined and verified. The apolipoprotein A1 (apoA1), as a contrast protein instead of apoB, was selected for nonspecific binding with the SERS-active immune substrate and the 4MBA-labelled immune nano-Au probes, and the test results are shown in Fig. 10. The characteristic SERS signal of 4MBA obtained from the contrast test (black line) is weak and similar to that of the background (red line), and far weaker than that of the specificity immunoassay of the apoB (blue line). Thus, nonspecificity was confirmed between the apoA1 and SERS-active immune substrate as well as the 4MBA-labelled immune nano-Au probes. Thus, on the basis of these data, our immunoassay protocol demonstrated good biological specificity.

4. Conclusions

A super-high-sensitivity immunoassay based on SERS was performed using nano-Au immune probes and the nano-Ag immune substrate for the quantitative and qualitative detection of apoB. In our experiment, an immunoassay of apoB was successfully performed for a range of concentrations from 200 pg/mL to 2 fg/mL, and the detection limit was as low as 2 fg/mL (3.878×10^{-18} mol/L). In the contrasting experiment, the SERS spectra corresponding to different target antigens were obtained under the same conditions. These results demonstrated that the nano-Au immune probes and the nano-Ag immune substrate exhibited not only strong SERS activity but also high biological specificity. Furthermore, the proposed immunoassay protocol can be used to detect other proteins also in addition to apoB. This

protocol displays potential for a super-high-sensitivity immunoassay and biochemical analysis.

Acknowledgements

This work was supported by the National Natural Science Foundation of China (Grant nos. 61036013, 61138003, 61275153, 61265009 and 61320106014), the Natural Science Foundation of Zhejiang (Grant no. LY12A04002), the International Collaboration Program of the Natural Science Foundation of Ningbo (Grant nos. 2010D10018 and 2012A610107), the K.C. Wong Education Foundation and the K.C. Wong Magna Foundation of Ningbo University, China.

References

[1] M. Fleischmann, P.J. Hendra, A.J. McQuillan, Chem. Phys. Lett. 26 (1974) 163–166.
[2] B. Sharma, R.R.A. Henry I., E. Ringe, R.P.V. Duyne, Mater. Today 15 (2012) 16–25.
[3] P.C. Lee, D. Meisel, J. Phys. Chem. 86 (1982) 3391–3395.
[4] C.S. Allen, G.C. Schatz, R.P.V. Duyne, Chem. Phys. Lett. 75 (1980) 201–205.
[5] H.X. Xu, J. Aizpurua, M. Käll, P. Apell, Phys. Rev. E 62 (2000) 4318–4324.
[6] A. Campion, P. Kambhampati, Chem. Soc. Rev. 27 (1998) 783–826.
[7] S.M. Nie, S.R. Emory, Science 275 (1997) 1102–1106.
[8] A. Michota, J. Bukowska, J. Raman Spectrosc. 34 (2003) 21–25.
[9] X.H. Huang, Ivan H. EI-Sayed, W. Qian, Mostafa A. EI-Sayed, Nnao Lett. 7 (2007) 1591.
[10] R.A. Alvarez-Puebla, David S. dos Santos , Ricardo F. Aroca, Analyst 132 (2007) 1210–1214.
[11] L. Rodriguez-Lorenzo, L. Fabris, R.A. Alvarez-Puebla, Anal. Chem. Acta 745 (2012) 10–23.
[12] Y.W.C. Cao, R.C. Jin, C.A. Mirkin, Science 297 (2002) 1536–1540.
[13] X.X. Han, G.G. Huang, B. Zhao, Y. Ozaki, Anal. Chem. 81 (2009) 3329–3333.
[14] J.D. Driskell, R.A. Tripp, Chem. Commun. 46 (2010) 3298–3300.
[15] Y.C. Cao, R. Jin, J.M. Nam, C.S. Thaxton, C.A. Mirkin, J. Am. Chem. Soc. 125 (2003).
[16] Y.L. Wang, H. Wei, B.L. Li, W. Ren, S.J. Guo, S.J. Dong, E.K. Wang, Chem. Commun. (2007) 5220–5222.
[17] Y. Cui, B. Ren, J.L. Yao, R.A. Gu, Z.Q. Tian, J. Raman Spectrosc. 38 (2007) 896–902.
[18] C.Y. Song, Z.Y. Wang, T.H. Zhong, J. Yang, X.B. Tan, Y.P. Cui, Biosens. Bioelectron. 25 (2009) 826–831.
[19] X.X. Han, B. Zhao, Y. Ozaki, Anal. Bioanal. Chem. 394 (2009) 1719–1727.
[20] S.P. Xu, X.H. Ji, W.Q. Xu, X.L. Li, L.Y. Wang, Y.B. Bai, B. Zhao, Y. Ozaki, Analyst 129 (2004) 63–68.
[21] N.L. Rosi, C.A. Mirkin, Chem. Rev. 105 (2005) 1547–1562.
[22] G.H. Gu, J.S. Suh, Langmuir 24 (2008) 8934–8938.
[23] W.Y. Li, P.H.C. Camargo, X.M. Lu, Y.N. Xia, Nano Lett. 9 (2009) 485–490.
[24] Z.Y. Wang, S.F. Zong, H. Chen, H. Wu, Y.P. Cui, Talanta 86 (2011) 170–177.
[25] X. Su, J.W. Zhang, L. Sun, T.W. Koo, S. Chan, N. Sundarajan, M. Yamakawa, A.A. Berlin, Nano Lett. 5 (2005) 49–54.
[26] M.D. Porter, T.J. Lipert, L.M. Siperko, G.F. Wang, R. Narayanan, Chem. Soc. Rev. 37 (2008) 1001–1011.
[27] X.X. Han, Y. Kitahama, T. Itoh, C.X. Wang, B. Zhao, Y. Ozaki, Anal. Chem. 81 (2009) 3350–3355.
[28] Z.Y. Jiang, X.X. Jiang, S. Su, X.P. Wei, S.T. Lee, Y. He, Appl. Phys. Lett. 100 (2012) 203104.
[29] G. Walldius, I. Jungner, J. Intern. Med. 259 (2006) 493–519.
[30] G.C. Zhu, Y.J. Hu, J. Gao, L. Zhong, Anal. Chim. Acta 697 (2011) 61–66.
[31] J. Martinez-Perdiguero, A. Retolaza, L. Bujanda, S. Merino, Talanta 119 (2014) 492–497.
[32] J. Turkevich, P.C. Stevenson, J. Hillier, Discuss. Faraday Soc. 11 (1951) 55–75.
[33] G. Mie, Ann. Phys. 25 (1904) 377–455.
[34] S. Basu, S.K. Ghosh, S. Kundu, S. Panigrahi, S. Praharaj, S. Pande, S. Jana, T. Pal, J. Colloid Interface Sci. 313 (2007) 724–734.
[35] S. Jang, J. Park, S. Shin, C. Yoon, B.K. Choi, M.-S. Gong, S.-W. Joo, Langmuir 20 (2004) 1922–1927.
[36] P. Galletto, P.F. Brevet, H.H. Girault, R. Antoine, M. Broyer, J. Phys. Chem. B 103 (1999) 8706–8710.
[37] Y. He, S. Su, T.T. Xu, Y.L. Zhong, J.A. Zapien, J. Li, C.H. Fan, S.T. Lee, Nano Today 6 (2011) 122–130.